Coulomb-nuclear interference with ^{6}Li: Isospin character of the 2_1^+ excitation in ^{70,72,74}Ge

M. D. L. Barbosa,[1] T. Borello-Lewin,[1] L. B. Horodynski-Matsushigue,[1] J. L. M. Duarte,[1] C. L. Rodrigues,[1] M. R. D. Rodrigues,[1] and G. M. Ukita[1,2]

[1]*Instituto de Física, Universidade de São Paulo, C.P. 66318, 05315-970, São Paulo, SP, Brazil*

[2]*Faculdade de Psicologia, Universidade de Santo Amaro, Rua Prof. Enéas de Siqueira Neto, 340, 04829-300, São Paulo, SP, Brazil*

(Received 27 May 2004; published 3 February 2005)

Ratios of $B(E2)$ to $B(IS2)$, that is, of the reduced quadrupole transition probabilities related, respectively, to charge and mass were extracted through Coulomb-nuclear interference (CNI) for the excitation of the 2_1^+ states in ^{70,72,74}Ge, with a relative accuracy of less than 4%. For this purpose, the CNI angular distributions associated with the inelastic scattering of 28-MeV incident ^{6}Li ions accelerated by the São Paulo Pelletron, and momentum analyzed by the Enge magnetic spectrograph were interpreted within the DWBA-DOMP approach (distorted wave approximation for the scattering process and deformed optical model for the structure representation) with global ^{6}Li optical parameters. The present CNI results demonstrate an abrupt change in the $B(E2)/B(IS2)$ ratio for ^{74}Ge: although for ^{70,72}Ge, values of the order of 1.0 or slightly higher were obtained, this ratio is 0.66 (7) for ^{74}Ge. The heavier Ge isotope is thus one of the few nuclei that, so far, have been shown to present clear mixed symmetry components in their ground-state band.

DOI: 10.1103/PhysRevC.71.024303 PACS number(s): 21.10.Re, 21.60.Ev, 27.50.+e, 24.10.Eq

I. INTRODUCTION

The chains of the Ge and Se isotopes, in the transitional mass region around $A = 70$, are especially well suited to be case studies in the attempt to clarify the role played by neutrons in defining the collective properties of low-lying excitations. The evolution, as a function of increasing A, of the $B(E2)$ values that characterize the first quadrupole excitation indicates in both chains a transition around $N = 40$, although the change is less pronounced for the Ge isotopes ($Z = 32$) than for the Se isotopes ($Z = 34$). Furthermore, focusing on the Ge chain, it is to be noted that the nucleus ^{72}Ge is one of the few nuclei in the periodic table that presents a 0^+ first excited state, possibly as a consequence of a shape coexistence phenomenon and/or as a shell effect due to the closure of the $N = 40$ subshell. Among other experimental evidence, two neutron transfer experiments (p,t) [1] and (t,p) [2] strongly suggest that neutrons are related to marked structure modifications in these isotopic chains.

In this context, it is to be stressed that $B(E2)$ values, which are the collective experimental quantities available in this region to date, provide information only about the proton contribution to the excitation, if polarization effects may be disregarded. Therefore, direct access to the reduced isoscalar transition probability $B(IS2)$ (mass) is also required, especially in transitional regions, where the importance of the neutrons is well documented and where it is inadequate to assume *a priori* that these excitations are dominated by simple homogeneous collective effects (relative contributions of protons and neutrons of about Z/N).

Angular distributions of the inelastic scattering cross sections of isoscalar projectiles, detailing the Coulomb-nuclear interference (CNI) region, are a particularly convenient means to put structure changes along isotopic chains into evidence [3]. In fact, when inducing the excitation of the first quadrupole state, these experiments allow for the simultaneous extraction of $B(IS2)$ and $B(E2)$, thus minimizing the uncertainty in the ratio between charge and mass reduced transition probabilities, since scale and some model uncertainties influence the ratio to a much lesser extent [3]. The most straightforward way of obtaining the desired information is to analyze the inelastic scattering data within a DWBA-DOMP approach (distorted wave approximation for the scattering process and deformed optical model for the structure representation), after verifying that the conditions imposed by the model are approximately met [3].

This paper refers to a CNI study of the inelastic scattering of ^{6}Li ($T = 0$), exciting the 2_1^+ states of ^{70,72,74}Ge. Values of the experimental ratios $B(E2)/B(IS2)$ have not been previously reported for the Ge chain. Although the literature presents several inelastic scattering studies employing isoscalar projectiles, specifically deuterons [4], α particles [5,6], and also ^{6}Li [7], none of these has measured and thereafter analyzed the CNI region.

II. EXPERIMENTAL PROCEDURE

In the $A \sim 70$ mass region, at bombarding energies suitable for stable operation of the São Paulo Pelletron accelerator, the lightest isoscalar projectile appropriate for CNI measurements is ^{6}Li. Exploiting the good beam characteristics of the accelerator and the properties of the Enge split-pole magnetic spectrograph, rather forward scattering angles can be observed, resulting in very discriminative angular distributions, if the bombarding energy is conveniently chosen.

The 28.0 MeV ^{6}Li beam of the São Paulo Pelletron accelerator was focused on uniform, isotopically enriched targets of ^{70,72,74}Ge, after passing defining slits of 1.0×2.0 mm^2. The self-supported, clean targets, with thicknesses of about 30 μg/cm^2 (^{70,72}Ge) and 60 μg/cm^2 (^{74}Ge), were prepared by well controlled electron bombardment evaporation of the elemental material. The ejectiles of the reaction were momentum analyzed by the spectrograph and detected

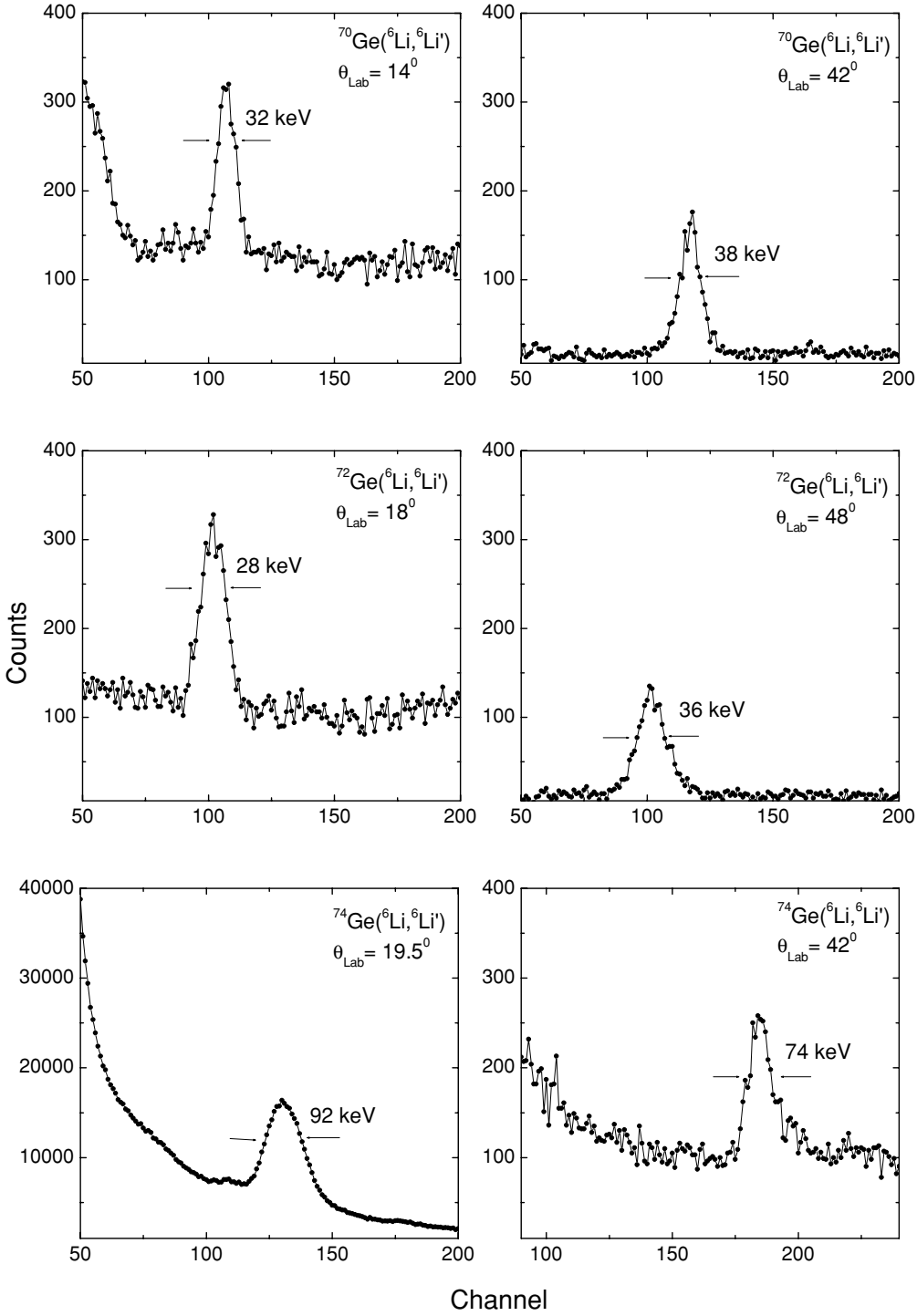

FIG. 1. Portions of position spectra showing the peak associated with inelastically scattered ^{6}Li ions after exciting the first quadrupole state in $^{70-74}$Ge.

by a 500-μm-thick surface barrier position-sensitive detector (PSD), with an area of 47 $\times$ 8 mm^2, positioned on the focal plane. During the experiment, elastically scattered ions of ^{6}Li were continuously monitored by a surface barrier detector fixed at $\theta_{Lab} = 27.5^{\circ}$. If in coincidence, the E (energy) and xE (position $\times$ energy) PSD signals, after analogic to digital conversion, are recognized as an event by the acquisition system (CAMAC). Through the division of those signals, the associated position spectrum was obtained. Figure 1 shows portions of the ^{6}Li position spectra for ^{70,72,74}Ge, displaying the respective 2_1^+ peak at some forward and intermediate scattering angles. An energy resolution of 30 to 40 keV was achieved in the ^{70,72}Ge spectra. A worse resolution, of about 70 to 90 keV, was observed for the ^{74}Ge spectra but did

TABLE I. Adopted optical model parameters [8].

Nuclei	V_0 (MeV)	r_R (fm)	a_R (fm)	V_I (MeV)	r_I (fm)	a_I (fm)	$r_C^{\rm b}$ (fm)
$^{70-74}$Ge	109.5	1.326	0.811	[a]	1.534	0.884	1.22

[a] $V_I = 58.16 - 0.328A + 0.00075A^2$, following the global prescription of Cook [8], resulting in 38.88 MeV (^{70}Ge), 38.43 MeV (^{72}Ge), and 38.00 MeV (^{74}Ge).

[b] r_C taken in accordance with [3] and references therein.

not interfere importantly in data analysis because the peak associated with the 2_1^+ excitation is isolated and better statistics were accumulated.

Relative normalization of the inelastic cross sections was obtained from the number of elastically scattered particles detected by the monitor during each run. The absolute normalization, for each isotope, was obtained from the fit of optical model predictions to the experimental elastic angular distributions, measured on the same target and under similar conditions. Shown in Table I are the global optical model parameters prescribed by Cook [8], which were employed in this normalization and also in the subsequent analysis; Figure 2 displays the experimental elastic angular distributions obtained for ^{70,72,74}Ge, in comparison with these predictions. Maximum scale uncertainties of $\pm 7\%$ for ^{70,72}Ge and of $\pm 10\%$ for ^{74}Ge are estimated, when contributions due to target nonuniformity and statistics in the elastic data are also considered.

III. ANALYSIS

Since the major interest is in the comparative evaluation of the contribution of protons and neutrons to the first quadrupole

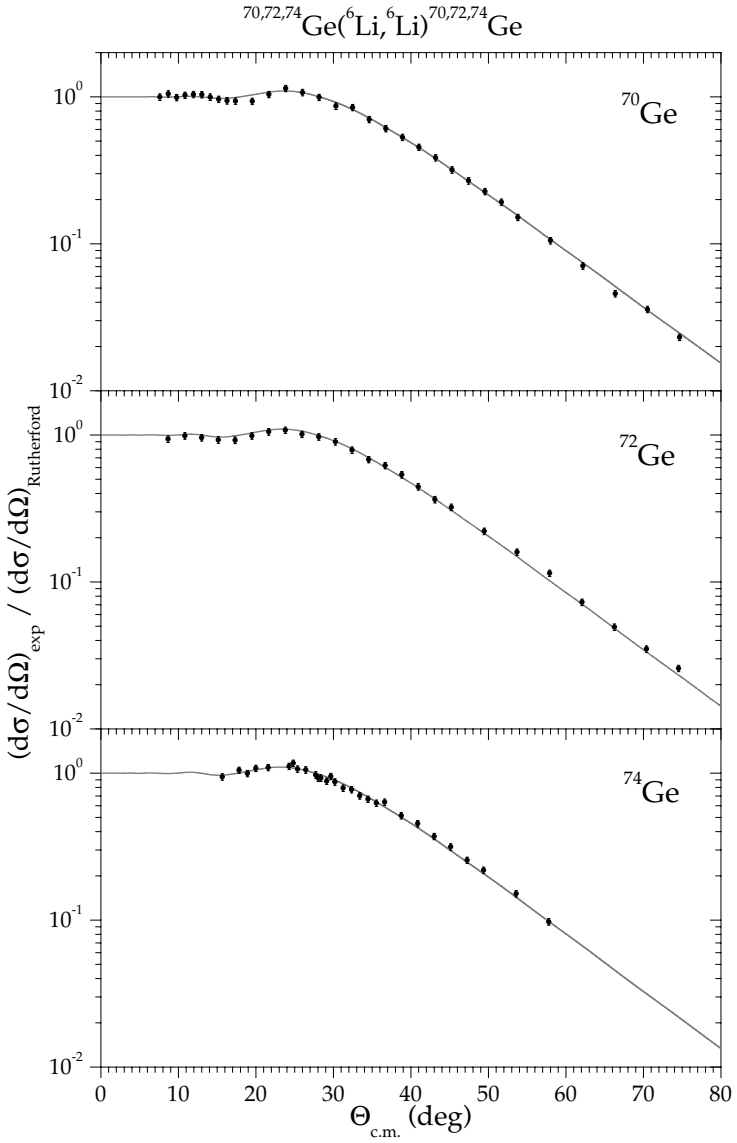

FIG. 2. Angular distributions of 28 MeV ^{6}Li, elastically scattered by $^{70-74}$Ge, and the optical model fit through the parameters of the global set of Cook [8]. Only random uncertainties are shown as error bars.

excitation along an isotopic chain, the DWBA-DOMP description [3], employing global optical model parameters, is an appropriate choice. In fact, this methodology allows for a very consistent and uniform analysis [3], whenever the underlying hypotheses are upheld by the experimental situation. This implies verifying initially whether the elastic scattering may be considered the dominant process. Due to the lower excitation energy and the higher $B(E2)$, the excitation of the 2_1^+ state in ^{74}Ge by ^{6}Li of 28.0 MeV was chosen as a test case to explore possible limitations in the analysis. Coupled channel calculations (using the CHUCK program) for this excitation, supposing equal deformation parameters for the nuclear and coulomb part and including couplings to the ground and quadrupole two-phonon states [6], reveal only minor changes in the angular distribution associated with the first 2_1^+ state, in comparison with the DWBA-DOMP predictions without recoil (code DWUCK4). Furthermore, perfect agreement between predictions, both those including and those not including recoil effects, was shown (codes Ptolemy x DWUCK4).

An important feature for comparative analyses is that in the DWBA-DOMP method the same parameters are used, not only to represent the incident and emergent distorted waves in the DWBA, but also to describe the transition potential within the DOMP approach [3]. In this approach, the effective transition potential responsible for the nuclear excitation is associated with the nonsphericities of the optical potential, whether these are dynamic or static ones, thus conveying an adequate parametrization for the intensity of the macroscopic effects. For convenience of the analysis, two parameters are chosen to characterize the collective excitation and are extracted through the comparison between predicted and experimental angular distributions: δ_2^N (mass deformation length, taken equal to the potential deformation length characterizing the transition) and C (defined as the ratio δ_2^C/δ_2^N, where δ_2^C is the charge deformation length). Although referring to a deformation of the potential well in the model, the parameter δ_2^N may be taken as a value characterizing the intensity of the collective excitation, whereas C is related to the relative importance of the proton contribution to this excitation. To keep free parameters under control it is of utmost importance to be able to choose a global optical model set for the DWBA-DOMP description. Such a set, although not much discussed in the literature, is available for ^{6}Li through the study of Cook [8], who analyzed a considerable amount of experimental data for $24 \leqslant A \leqslant 208$, in the incident energy range of 13–156 MeV. Those global parameters have provided very satisfactory fits in the analysis of ^{6}Li elastic and inelastic data, both in the Ru [9] region and the Ge region [10].

Detailing the ingredients of the analysis, the nuclear and Coulomb form factors are, respectively,

$$F_2^N(r) = -\,\delta_{R,2}^N(U)\,\frac{dV_0(r)}{dr} - i\,\delta_{I,2}^N(U)\,\frac{dV_I(r)}{dr}, \tag{1}$$

$$F_2^C(r) = \begin{cases} \dfrac{4\pi\,Z_a e}{5\,r^3}\,[B(E2)]^{1/2}, & \text{for } r \geqslant R_C \\ 0, & \text{for } r < R_C, \end{cases} \tag{2}$$

where V_0 and V_I are the real and imaginary parts of the optical potential U, following the standard Woods-Saxon dependences with given geometrical parameters (r_R, a_R and r_I, a_I); $Z_a = 3$ is the charge of the projectile; $R_C = r_C\,A^{1/3}$ is the sharp cutoff radius of the charge distribution; and $F_2^C(r)$ is taken to be equal to zero outside R_C without harm, since the reaction occurs peripherally.

The reduced electric transition probability $B(E2)$ for the quadrupole excitation starting from the ground state is given by

$$B(E2) = \left(\delta_2^C\right)^2 \left[\frac{3ZR_c}{4\pi}\right]^2 e^2, \tag{3}$$

where δ_2^C is the charge deformation length associated with the usual charge deformation parameter scaled by the charge radius R_C [11].

In the analysis, the real and imaginary potential deformation lengths are taken to be equal and determine the mass deformation length of the target nuclei for an undeformed projectile: $\delta_2^N = \delta_{R,2}^N(U) = \delta_{I,2}^N(U)$.

In analogy with expression (3), the isoscalar deformation length (mass), δ_2^N, is related to $B(IS2)$ through the expression

$$B(IS2) = \left(\delta_2^N\right)^2 \left[\frac{3ZR_m}{4\pi}\right]^2, \tag{4}$$

considering in this definition the scaling through Z, as proposed by Bernstein *et al.* [12], with $R_m = r_m\,A^{1/3}$, the mass radius. Adopting this definition, if $\delta_2^N = \delta_2^C$ (meaning a homogeneous collective quadrupole excitation), the mass (or isoscalar) reduced transition probability turns out to be numerically almost equal to the electric one.

The ratio $B(E2)/B(IS2)$ is, therefore, proportional to the square of the parameter C, that is to $(\delta_2^C/\delta_2^N)^2$. Taking the adopted definition of $B(IS2)$ and considering neutron and proton transition densities as proportional to each other, the ratio of the quadrupole moments of the neutron and proton distributions can be written as

$$\left|\frac{M_n}{M_p}\right| = \frac{A}{Z}\left|\frac{B(IS2)}{B(E2)/e^2}\right|^{1/2} - 1 = \frac{A}{Z}\left(\frac{r_m}{r_c}\right) C^{-1} - 1. \tag{5}$$

Note that $C \sim 1$ corresponds to the homogeneous collective excitation, in which neutrons and protons contribute in the ratio of their numbers.

The discriminative power of the CNI method in the mass region of interest can be appreciated through inspection of Figs. 3 and 4, as a function of the ^{6}Li beam energy. Both Fig. 3 and Fig. 4 show DWBA-DOMP predictions (DWUCK4 [13]) for the ^{74}Ge($0_1^+ \rightarrow 2_1^+$) excitation, again taken as an example. The separated and combined nuclear and Coulomb contributions are represented in Fig. 3, taking $C = 1$, for four chosen incident energies of 22, 28, 32, and 36 MeV, where the extreme values are approximately the limits of the tandem for this application. It is seen that to produce an appreciable interference effect in the scattering of ^{6}Li on Ge isotopes, the incident energy should be 28 MeV or above. Figure 4 displays, for the same incident energies, the effect of a range of values of C on the angular distribution shape, comparing the changes produced in the interference pattern. Following these findings, the incident energy of 28 MeV was preferred in the present work, since measurements near the interference minimum

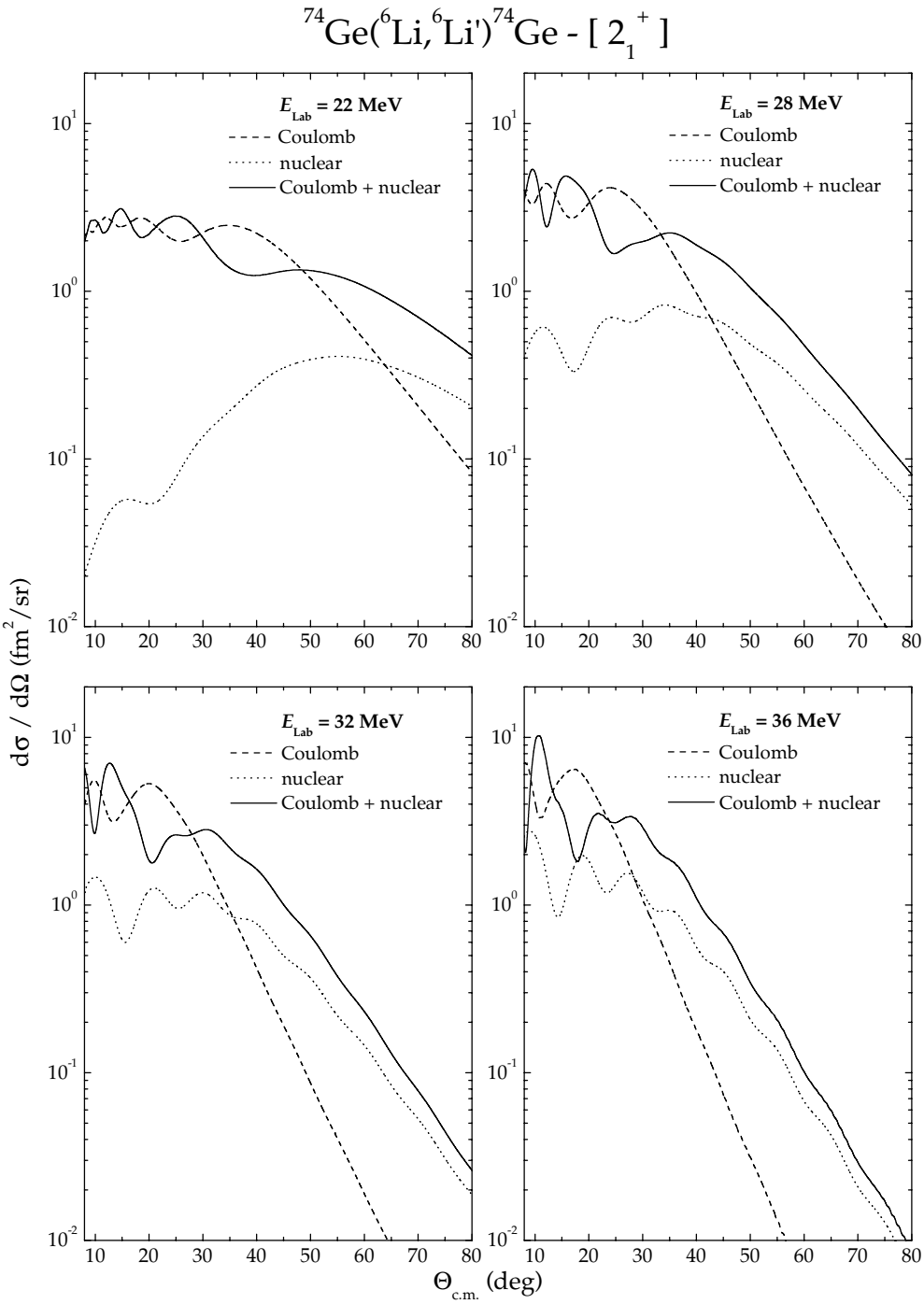

FIG. 3. Coulomb and nuclear contributions and their combined effect on the predicted DWBA-DOMP angular distributions of the ^{6}Li inelastic scattering exciting the first quadrupole state of ^{74}Ge, as a function of incident energy.

at $\theta_{c.m.} \sim 12.5^\circ$ are still accessible with the spectrograph, contributing to C discrimination.

IV. RESULTS

The DWBA-DOMP predictions without recoil effects (DWUCK4 program [13]), using the global optical model parameters of Cook [8], were fitted to the data through the Gauss-Marquardt [3] procedure, adjusting the parameters δ_2^N and C, to minimize χ^2. To account for the range of scattering angles ($\theta \pm \Delta\theta$) that are admitted through the spectrograph solid angle in the center of mass system, the predicted values have been integrated numerically in this range. The experimental angular distributions associated with the first 2^+ excitations, respectively, in ^{70,72,74}Ge, and the resulting fits are shown in Fig. 5. The best fit parameters C and δ^N extracted,

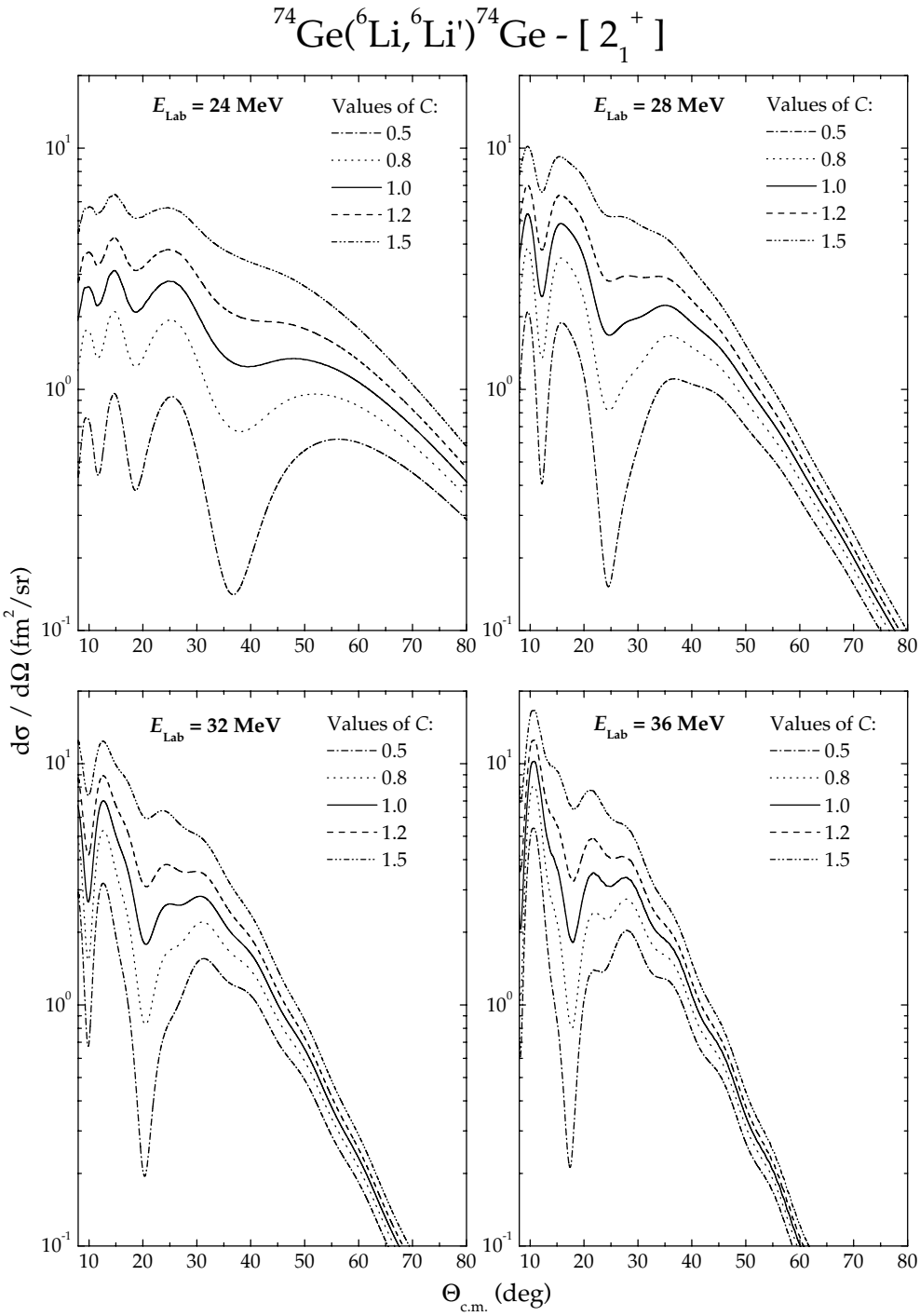

FIG. 4. The effect of diverse values of C on the predicted angular distribution of ^{74}Ge(^{6}Li,^{6} Li′)^{74}Ge[2_1^+], as a function of incident energy.

the corresponding statistical uncertainties, and the values of the reduced χ^2 are also presented in Fig. 5. To assess the sensibility of the procedure, the predicted angular distributions obtained when the C values are increased or decreased by 0.100 are also shown.

To illustrate the statistical adequacy of the method [3], Fig. 6 presents the results of Monte Carlo (MC) simulations projected onto the plane of the adjusted parameters (C,δ^N) for ^{70}Ge (6a) and ^{74}Ge (6b). Constant χ^2 contour lines, corresponding to some usual confidence levels are also shown. In each of these MC simulations, 10,000 "new sets of experimental points" (each set constituting a "new" angular distribution) were generated by randomly choosing from a Gaussian distribution of cross section values, with given standard deviation, around each measured point. Each of these simulated sets of data points underwent a fitting procedure that resulted in a "simulated" DWBA-DOMP angular distribution, characterized by "new" values of (C, δ^N), for which the corresponding χ^2

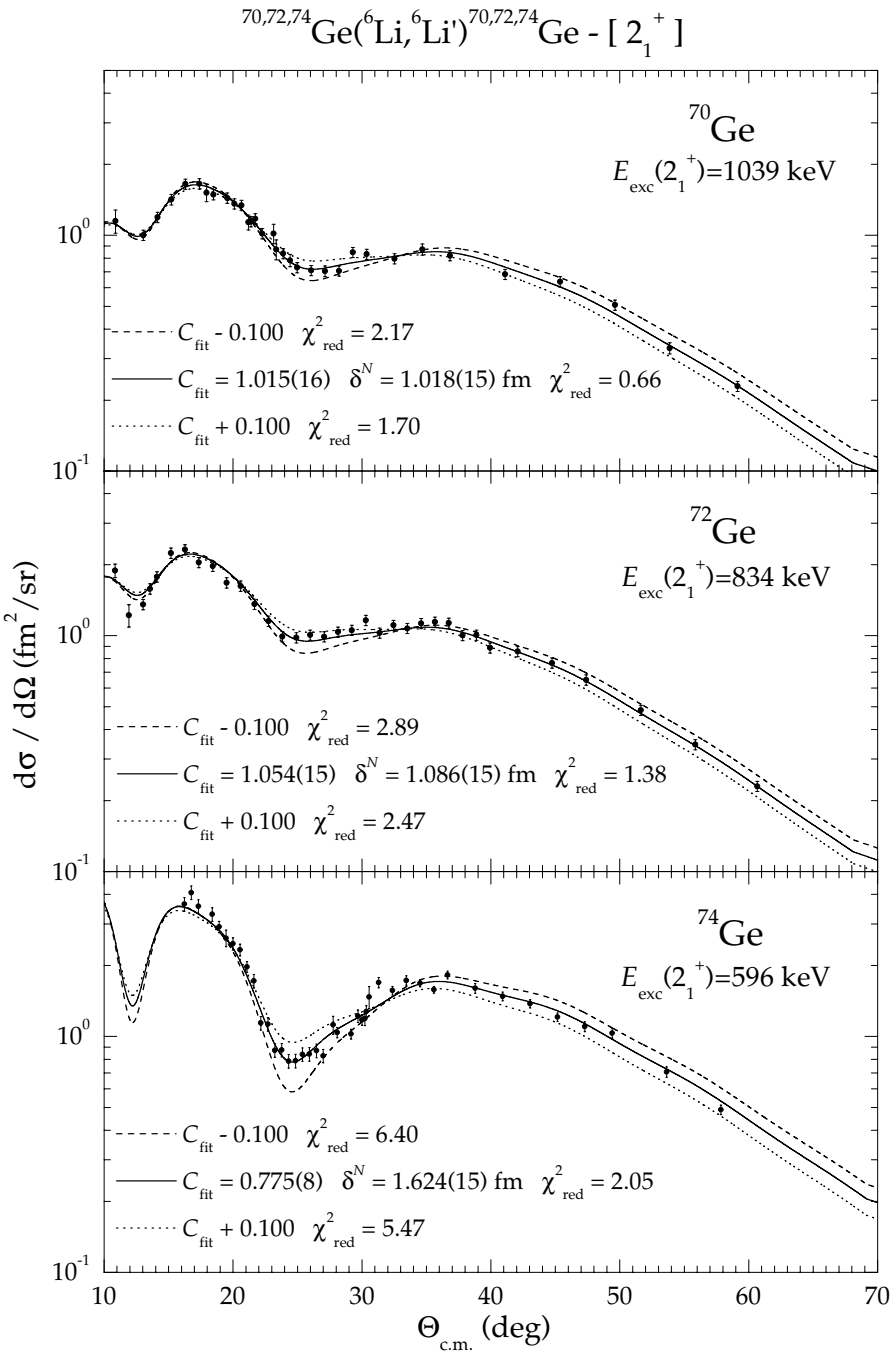

FIG. 5. Experimental angular distributions of the inelastic scattering of ^{6}Li, exciting the first quadrupole state in ^{70,72,74}Ge, and their fit through the DWBA-DOMP approach with global optical parameters. For each isotope, the best fit is shown as a continuous line; the minimum value of $\chi^2_{\rm red}$ and the adjusted parameters are presented; and the effect of modifying C by ± 0.100 is ilustrated by the dashed and dotted lines. Only random uncertainties are shown as error bars and given as uncertainties for δ^N.

was obtained by comparison with the original experimental angular distribution. Figures 7 and 8 display, respectively, for ^{70}Ge and ^{74}Ge, this χ^2 surface, where each point represents the (δ^N, C, χ^2) values of one "simulated" DWBA-DOMP fit on one MC trial, from two different perspectives. As can be appreciated from Fig. 9, the χ^2 contour lines obtained through the MC simulations are almost perfect ellipses, in very good agreement with the outcomes of the Gauss approximation (GA) employed in the analysis, for both the ^{70}Ge (9a) and ^{74}Ge (9b) results. Figures 6 and 8 demonstrate that the experimental angular distribution for the heavier Ge isotope does not admit any fit that could result in values of C and δ^N closer to those of ^{70,72}Ge (2^+_1). In fact, the angular distribution of ^{74}Ge(^{6}Li, ^{6}Li$'$) is distinctly different from those of ^{70,72}Ge (see Fig. 5).

Finally, Table II summarizes the results of this experiment for the first quadrupole excitations in ^{70,72,74}Ge. The uncertainties in the C values follow directly from the statistical analysis discussed above, whereas those for δ^N_2 also include the contribution of the cross section scale uncertainty for each isotope. Also shown in Table II are the ratios $B(E2)/B(IS2)$, calculated using the values [3] $r_C = 1.22$ fm and $r_m = 1.16$ fm, respectively, for the reduced radii of the equivalent sharp cutoff uniform charge and mass distributions. If an uncertainty of

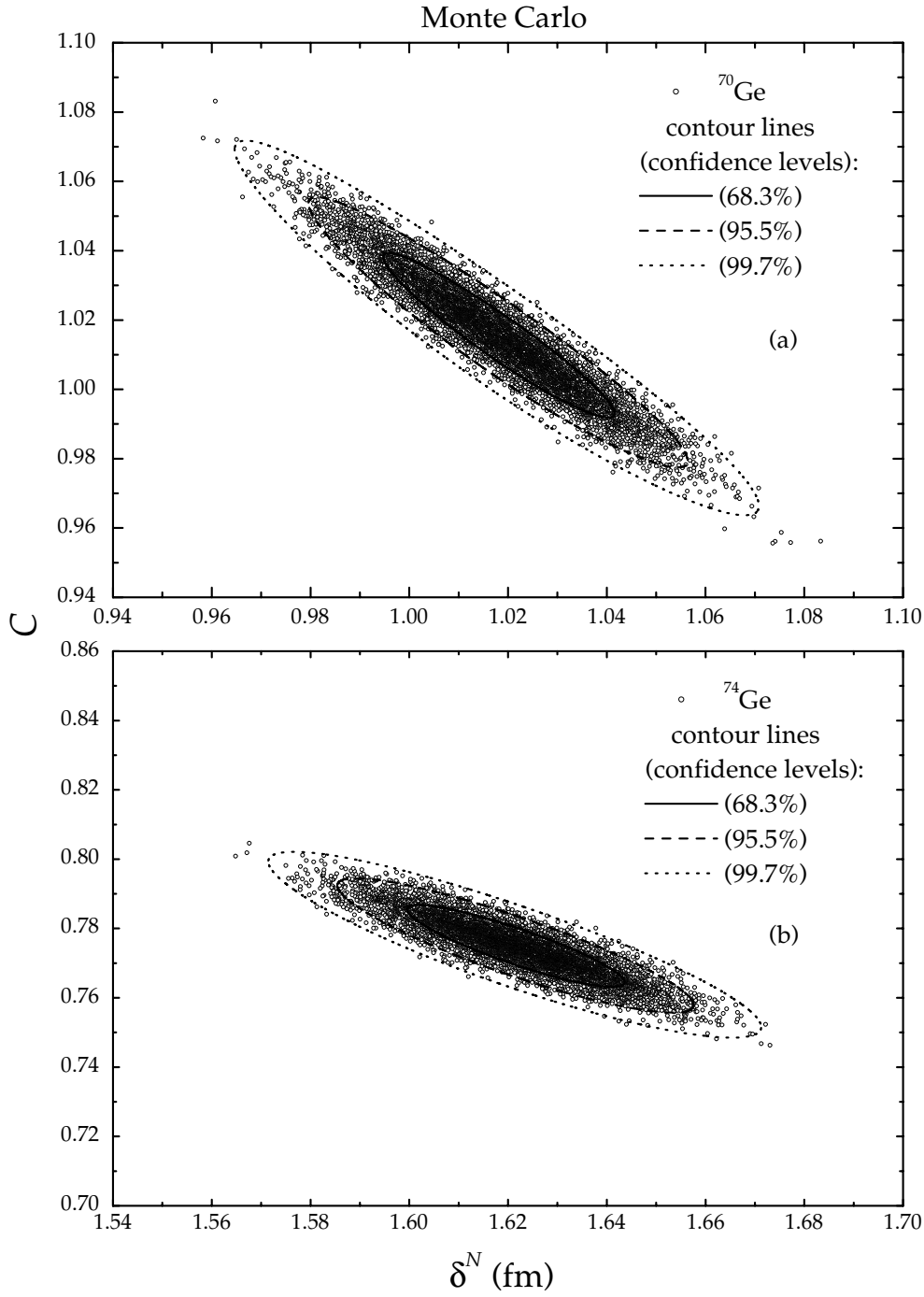

FIG. 6. Monte Carlo simulated results for ^{70}Ge (a) and ^{74}Ge (b). Also shown are the uncertainty intervals corresponding to some usual confidence levels, bounded by constant χ^2 contour lines (CL).

$\pm 5\%$ is associated with the ratio r_c/r_m, $\pm 10\%$ should be added quadratically to the uncertainties quoted for the $B(E2)/B(IS2)$ values, which is then responsible for the predominant contribution to the total uncertainty in those values. These composed uncertainties are to be employed if the values in Table II are to be compared to other experimental results. It is to be stressed, on the other hand, that comparisons of the ratio between the three isotopes here studied are to be made within the quoted uncertainties. No uncertainty was deliberately attributed to $|Mn/Mp|$ because model inadequacies probably play the greater part in the extraction of this ratio; however, only by propagation of the uncertainties associated with the quantities in expression (5) is an uncertainty of more than 10% expected.

As can be appreciated with the help of Table II, the values of C are almost the same for ^{70}Ge and ^{72}Ge, but

TABLE II. Results of the present experiment—parameters C and δ_2^N extracted for the first quadrupole excitation in ^{70,72,74}Ge. Also presented are the values of the ratios $B(E2)/B(IS2)$, $|Mn/Mp|$, derived from the values of C, and N/Z.

A	C	δ_2^N[a] (fm)	$B(E2)/B(IS2)$[b] (e^2)	$\lvert M_n/M_p\rvert$[c]	N/Z
70	1.015 (16)	1.02 (4)	1.140 (35)	1.05	1.19
72	1.054 (15)	1.09 (4)	1.228 (35)	1.03	1.25
74	0.775 (8)	1.62 (8)	0.664 (14)	1.84	1.31

[a]Uncertainties include estimated systematic scale uncertainties.
[b]For comparisons with other experimental results, ±10% should be quadratically added to the uncertainties (see text).
[c]Uncertainties of at least 10% (see text).

an abrupt change is detected in going to ^{74}Ge, clearly indicating a predominant contribution of the neutrons to the first quadrupole excitation of this isotope. As a consequence, the ratio $B(E2)/B(IS2)e^2$, similar for ^{70}Ge and ^{72}Ge, decreases significantly for ^{74}Ge. For the extracted mass deformation lengths, a strong increase is detected in ^{74}Ge, and therefore in $B(IS2)$, as compared with similar values obtained for ^{70,72}Ge.

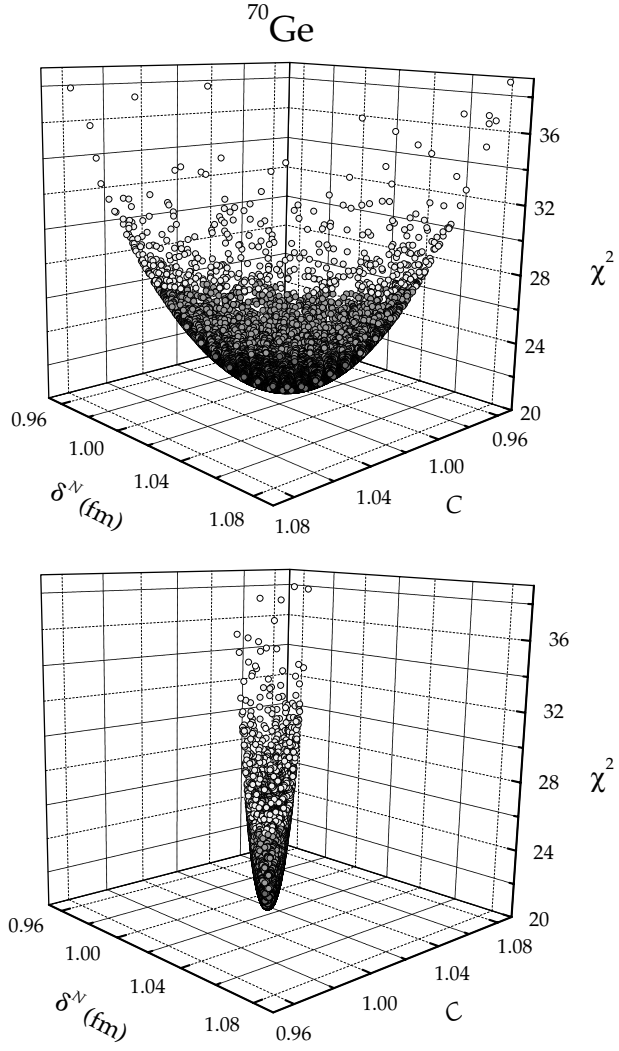

FIG. 7. Two views of the χ^2 distribution of 10^4 Monte Carlo simulated results corresponding to the parameters δ^N and C, obtained in the fit to randomly chosen values around the experimental points of the actual angular distribution for ^{70}Ge(^{6}Li,^{6}Li′)^{70}Ge[2_1^+].

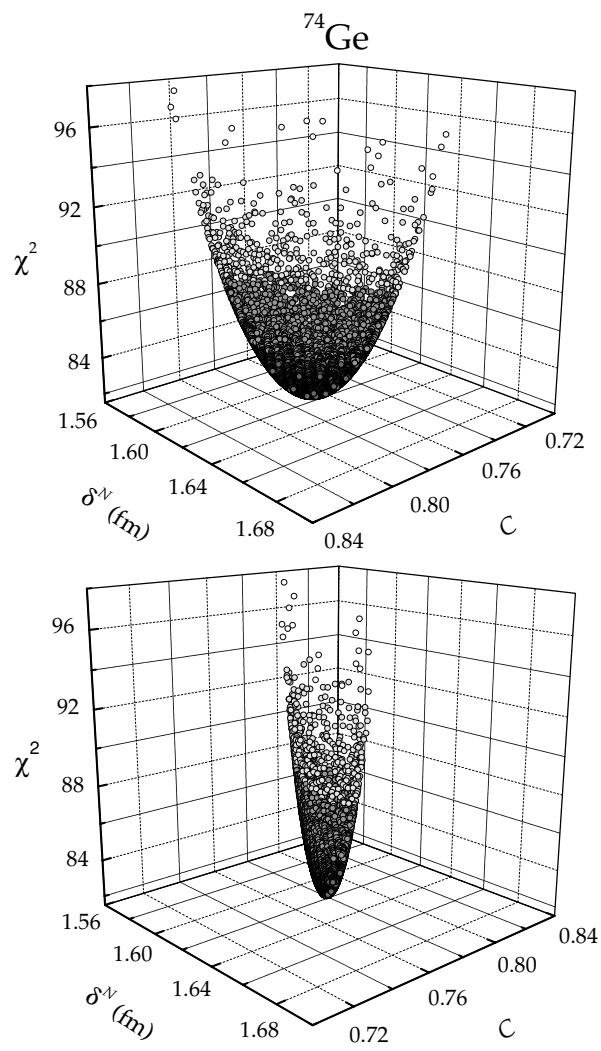

FIG. 8. Two views of the χ^2 distribution of 10^4 Monte Carlo simulated results corresponding to the parameters δ^N and C, obtained in the fit to randomly chosen values around the experimental points of the actual angular distribution for ^{74}Ge(^{6}Li,^{6}Li′)^{74}Ge[2_1^+].

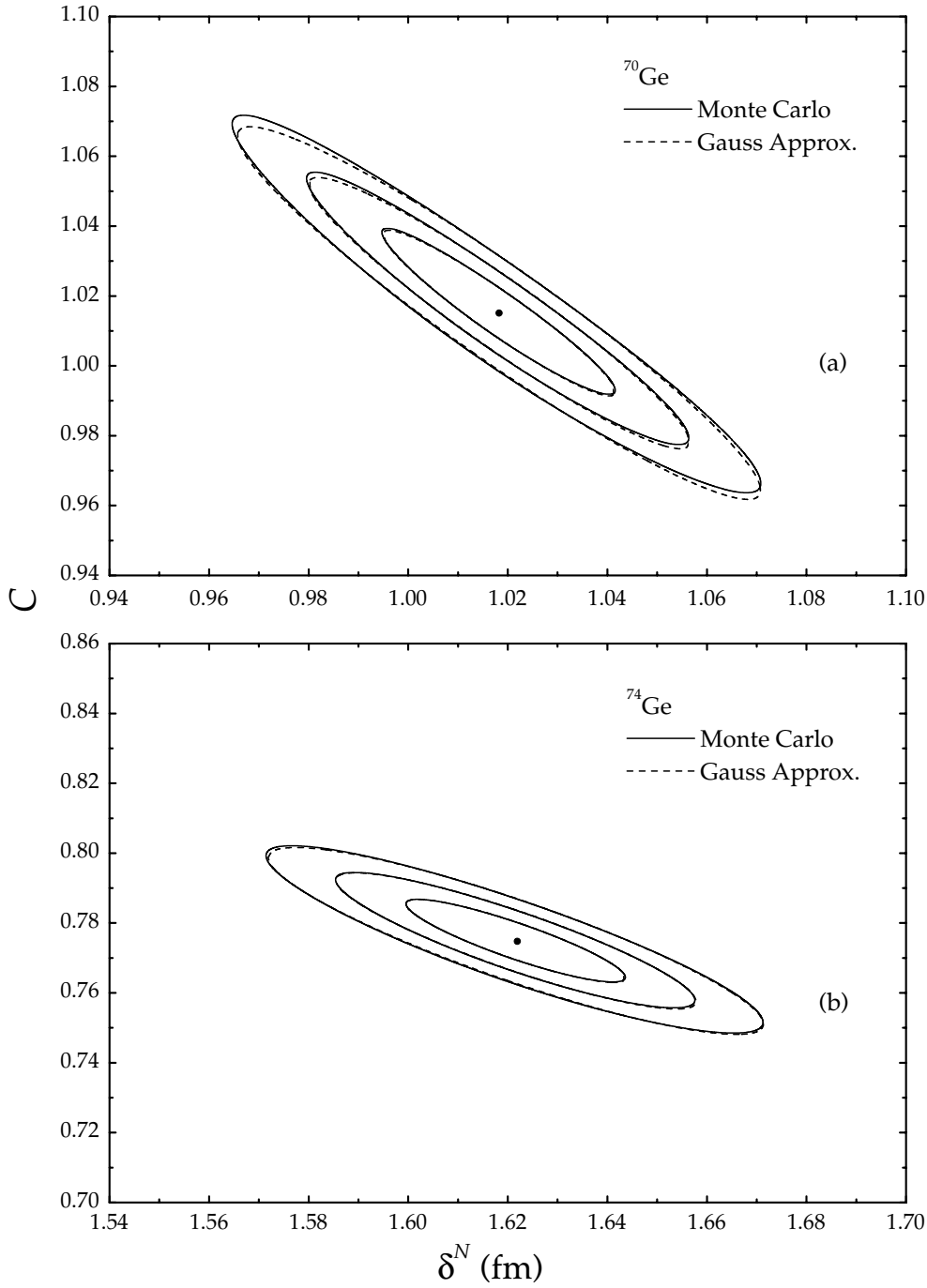

FIG. 9. Comparison between the outcomes of the Monte Carlo simulations, characterized by the constant χ^2 contour lines and the respective Gauss approximation ellipses, both corresponding to the 68.3%, 95.5%, and 99.7% confidence intervals: ^{70}Ge (a) and ^{74}Ge (b).

The role played by the neutrons relative to the protons in these excitations can also be characterized through the comparison of N/Z, expected from the homogeneous collective model, with the experimental $|M_n/M_p|$. Table II shows that the values of $|M_n/M_p|$ are 11% and 18% smaller than N/Z, respectively for $A = 70$ and 72, and characterizing the transition in $A = 74$, for this isotope the experimental value is, on the contrary, 40% higher than the prediction of the homogeneous collective model.

For the charge deformation lengths, deduced from the adjusted parameters C and δ_2^N, a smoothly increasing trend emerges as a function of mass number A. The trend for δ_2^C starting from the adopted $B(E2)$ values [11], although also showing a monotonic increase of δ_2^C as a function of A,

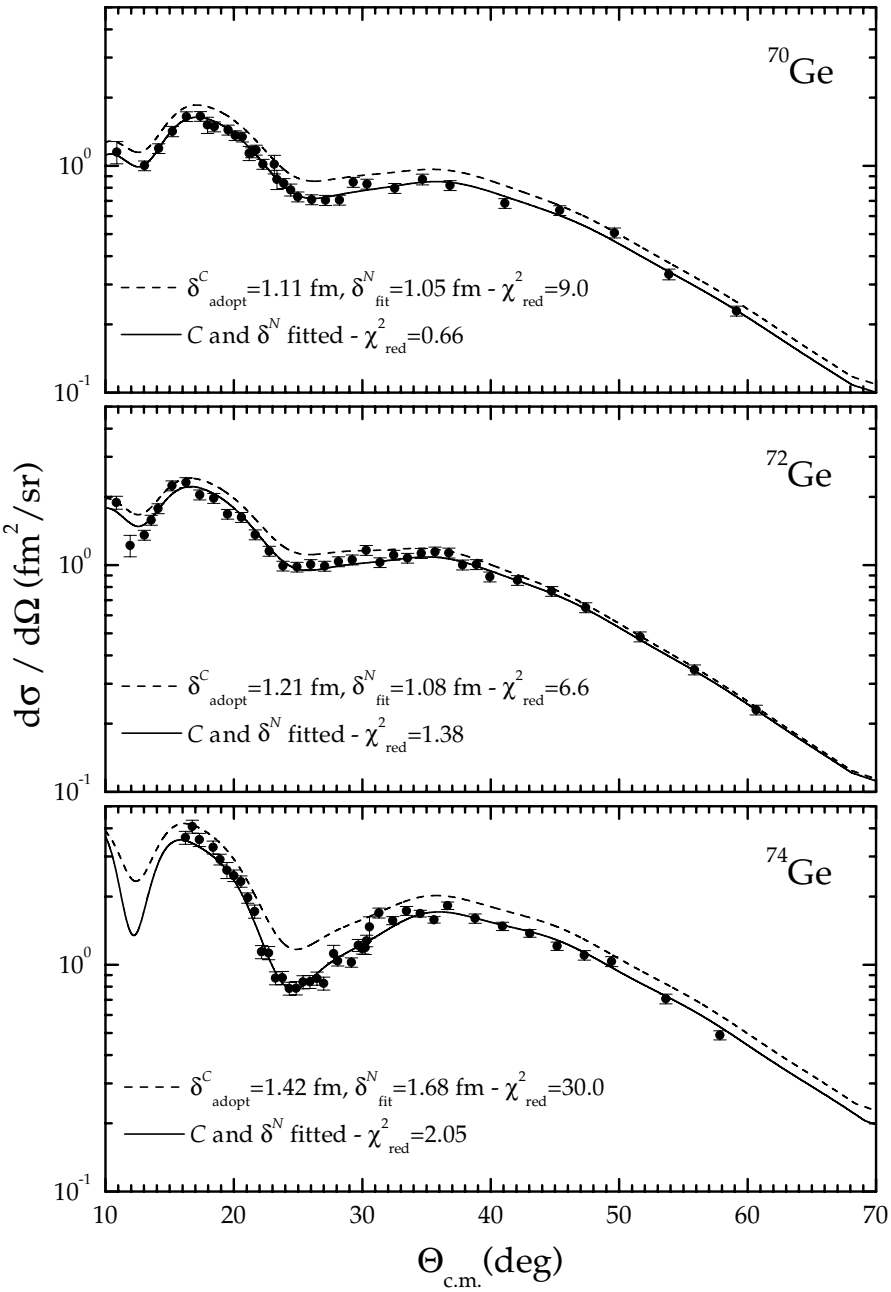

FIG. 10. Experimental angular distributions of ^{70,72,74}Ge(^{6}Li, ^{6}Li′)^{70,72,74}Ge[2^+_1] in comparison with their best fit and with the fits obtained by imposing the values of the respective $B(E2)$ taken from the literature [11]. Note that systematic scale uncertainties (see Sec. II) have to be considered in comparisons.

reveals a change of behavior between $A = 72$ and $A = 74$ with an increase of 17%, compared to a 9% increase between $A = 70$ and $A = 72$. Figure 10 shows the comparison of the experimental angular distributions for $A = 70, 72$, and 74, with two DWBA-DOMP predictions. One prediction corresponds to the best fit to the data, and the other is calculated by imposing the δ_2^C values extracted from the adopted $B(E2)$ [11], while allowing only the δ_2^N parameter to vary. It is seen that, as expected, the fit with two free parameters is superior to the one with a fixed value of δ_2^C. It is, further, apparent that the χ^2_{min} values would be much lower if the cross sections were increased by a factor of about 1.15, somewhat outside the experimental uncertainties. However, the experimental values for C obtained in the fit of worse quality still confirm the main finding of the present work: C values are greater than 1.0 and are increasing between ^{70}Ge and ^{72}Ge, whereas C is consistently smaller than 1.0 for ^{74}Ge, indicating predominance of the neutrons. It is, further, to be stressed that scale uncertainties (see Sec. II) should be considered in the comparisons of δ_2^N (see Table II).

Previous CNI work of the São Paulo group [14,15] had already shown that the first quadrupole excitation in several nuclei in the $A \sim 100$ mass region is characterized by values of $C \geqslant 1.0$, whereas the Zr isotopes with $Z = 40$ and

$N = 52, 54, 56$ also show a definite predominance of the neutrons in this excitation [16,17].

V. DISCUSSION AND CONCLUSION

The nuclei in the $Z \sim 30$, $N \sim 40$ region, although at the center of interest for about three decades, still pose some intriguing questions, associated in particular with discontinuities in several experimental indicators along isotopic chains [18]. One of the most prevalent methods of tackling these questions has been to introduce a two-state coexistence model of some kind. The basic idea behind this interpretation is to assume the existence of two orthogonal "unperturbed" configurations, φ_g and φ_e, which may coexist and mix in different proportions to form the physical states observed. This model was triggered in particular by the peculiar behavior of the 0_2^+ state in this mass region and was started in the mid-1970s for the Ge isotopes, for which the mixing states were interpreted as differing only in their proton configurations [19]. Two-neutron transfer experiments [1,2] soon showed the inadequacies of this interpretation, which was experimentally dismissed for ^{72}Ge in 1987 by the two-proton transfer study of Fortune *et al.* [20]. A so-called generalized two-state model was introduced in 1984 by Carchidi *et al.* [21], which not only explained the (p,t) and (t,p) results [21,22], but also had considerable success in interpreting [23] several of the other discontinuities, such as those observed in α pickup and stripping. In this model only very general assumptions were made about the configuration φ_g, which was associated predominantly with the ground state of the lighter Ge isotopes, and about the configuration φ_e, which was associated predominantly with the corresponding excited 0^+ level, considered an intruder state. However, as clearly demonstrated in the 1984 work [21], a necessary consequence of this model is an interchange of the predominance between φ_g and φ_e, respectively in the physical ground and excited 0^+ states, in going from ^{70}Ge to ^{76}Ge, the transition occurring most probably between ^{72}Ge and ^{74}Ge.

On the other hand, in the early 1980s, the existence of a shape transition and of shape coexistence in even-A germanium nuclei had seemed to be clearly indicated by the comparison of experimental data obtained in Coulomb excitation [24,25] and two-neutron transfer reaction measurements [2,26,27]. From the experimental static quadrupole moment Q_{2^+} and $B(E2)$ values, associated with the first quadrupole excitation, an almost spherical nature had been assigned to the ^{70}Ge and ^{72}Ge ground states, whereas a moderately deformed nature had been instead attributed to the ground states of ^{74}Ge and ^{76}Ge [24,28]. Indeed, in line with the findings obtained via the electromagnetic interaction, the analyses of the $L = 0$ transfers in both (t,p) and (p,t) reactions had shown that the transition strengths between the ground states of similar nature, $^{70}\text{Ge} \rightleftharpoons {}^{72}\text{Ge}$ and $^{74}\text{Ge} \rightleftharpoons {}^{76}\text{Ge}$, are larger than those between the ground states of ^{72}Ge and ^{74}Ge [2,26,27].

This interpretation of Lecomte *et al.* [28] did not, in principle, contradict the generalized two-state model. In fact, in the later 1980s Fortune and Carchidi [18] were able to include all existing Coulomb excitation information into their generalized two-unperturbed-state model, concluding that for ^{70,72}Ge each one of the two lowest lying 2^+ states is relatively pure, and especially in ^{72}Ge, neither of them is appreciably connected to φ_e. As for the 0^+ levels, that work [18], which was based on the more extensive data set for ^{70,72}Ge, obtained a 71% and 62% predominance of φ_g in their respective physical ground states, whereas it determined upper limits of only 14% and 5%, respectively, for φ_g in those of ^{74,76}Ge, confirming the prediction that the interchange of structure between ground and excited 0^+ levels should occur in going from ^{72}Ge to ^{74}Ge; the physical 2_1^+ levels would then be connected to the ground states in ^{74,76}Ge exclusively by their φ_e amplitudes.

Difficulties for the extremely nice picture thus constructed arose when it became clear, through extensive multiple Coulomb excitation experiments [29–31], that the physical 0_2^+ showed characteristics of a rather spherical structure, not only in ^{72}Ge, but also, in a very similar manner, in both ^{74}Ge and ^{76}Ge, whereas in the sequence of $A = 70 - 76$ the 2_1^+ level is connected to the physical ground state through rather intense, not extremely different, $B(E2)$ values of, respectively, 21, 24, 33, and 29 single particle units [24]. Kotlinski *et al.* [29] obtained for the φ_g configuration in ^{72}Ge a very good accord with an asymmetric rotor model with $\gamma = 28.5^\circ$, although the positive static quadrupole moment of the 2_2^+ level, interpreted as the head of the γ band, resulted in only about half the experimental value. Of course, no further information on the 0_2^+ intruder component was obtained within this interpretation. The recent studies of both ^{74}Ge [30] and ^{76}Ge [31], with techniques similar to those of the ^{72}Ge one [29], concluded for the existence of structures that are rather similar to those of ^{72}Ge, there is a ground-state band, associated with prolate characteristics; a band based on the 2_2^+ level, with a positive Q value close to 0.3 eb; and a coexisting spherical structure for the 0_2^+.

Only very recently another extensive multiple Coulomb excitation study [32], focusing on the ^{70}Ge isotope, became available. In contrast with what similar techniques had revealed in other mass regions, where rather smooth transitions between two competing shapes were uncovered [33], it is now clear that at least three different configurations must be competing in the Ge region [32]. Analyzing results for the $N = 38$ isotones, ^{72}Se and ^{74}Kr, as well, Sugawara *et al.* [32] suggest that the competing configurations in ^{70}Ge are, on the one hand, axially asymmetric or near oblate; on the other hand, spherical; and finally, near prolate. In this interpretation, the ground states of both the $Z = 32$ isotopes (with $70 \leqslant A \leqslant 76$) and the $N = 38$ isotones (with $70 \leqslant A \leqslant 74$) would be predominantly axially asymmetric with a nearby spherical configuration mixing in, especially for ^{72}Ge. The prolate shape would also be competing in most of these nuclei, being absent only in ^{74,76}Ge. In fact, the situation may be still more complex, since it is not obvious how the two-neutron transfer results [18] could be accommodated in this picture, and no attempt to do so has been published by Sugawara *et al.* [32].

The present study may be contributing to solving the puzzle of the Ge nuclei by adding yet another piece, because besides being axially asymmetric, the ground state of ^{74}Ge may, for instance, be "softer" in its neutron degree of freedom than it is in its proton one. It is to be remembered that, even if there is configuration mixing in the ground state, the inelastic

scattering would excite only that configuration that connects the ground and 2_1^+ states of each isotope, because the 2_1^+ states turn out rather pure [18,32]. The most important outcome of the present work is, therefore, that, as revealed by the experimental ratios $B(E2)/B(IS2)e^2$ (or, alternatively, by $|M_n/M_p|$), the role played by the neutrons relative to the protons in the first quadrupole excitation is strongly enhanced in ^{74}Ge in comparison with ^{70}Ge and ^{72}Ge. In ^{70}Ge, almost the usual contribution of N/Z is detected and in ^{72}Ge there is a slight predominance of the protons.

The IBM-2 interpretation of the $A \sim 70$ region, in particular also of the Ge chain [34], available in the literature simply fixes, as usual, the boson charges to fit the experimental $B(E2; 2_1^+ \rightarrow 0_1^+)$ value and takes no $B(IS2)$ value into account. The only existing IBM-1 analysis [35] admitted the breaking of one boson, but even so it was clearly unable to improve the level of agreement with experimental data. Dynamic deformation theory [1,36] had formerly predicted a shape transition between ^{72}Ge (G.S.) and ^{74}Ge (G.S.).

It would be interesting to see if the proton and neutron boson version (IBM-2) could provide an interpretation of the present results, demonstrating different F-spin admixtures [37] in the 2_1^+ states along the Ge chain. In fact, this complex transitional mass region could elude even these attempts at understanding the underlying nuclear structure, since there are experimental clues, such as very low-lying $7/2^+$ levels [38] (that even become ground states in the $N = 45$ isotones ^{77}Ge, ^{79}Se, ^{81}Kr, ^{83}Sr, and ^{85}Zr and possibly other nuclei of the region), which point to the necessity of at least a broken pair approach.

As a next step in the study of the Ge chain, measurements of CNI in the inelastic scattering of ^{6}Li on ^{76}Ge, with the aim of comparing the relative contributions of protons and neutrons in the transition to the first quadrupole state in this isotope with those here determined for ^{74}Ge, are clearly of interest.

ACKNOWLEDGMENTS

This work was partially supported by Fundação de Amparo à Pesquisa do Estado de São Paulo (FAPESP) and Conselho Nacional de Desenvolvimento Científico e Tecnológico (CNPq).

[1] D. Ardouin, C. Lebrun, F. Guilbault, B. Remaud, E. R. Flynn, D. L. Hanson, S. D. Orbesen, M. N. Vergnes, G. Rotbard, and K. Kumar, Phys. Rev. C **18**, 1201 (1978).
[2] C. Lebrun, F. Guilbault, D. Ardouin, E. R. Flynn, D. L. Hanson, S. D. Orbesen, R. Rotbard, and M. N. Vergnes, Phys. Rev. C **19**, 1224 (1979).
[3] J. L. M. Duarte, G. M. Ukita, T. Borello-Lewin, L. B. Horodynski-Matsushigue, and L. C. Gomes, Phys. Rev. C **56**, 1855 (1997).
[4] S. Sen, S. E. Darden, R. C. Luhn, N. O. Gaiser, G. Murillo, and J. Ramirez, Phys. Rev. C **31**, 787 (1985).
[5] F. Ballester, E. Casal, and J. B. A. England, Nucl. Phys. **A490**, 227 (1988).
[6] L. H. Rosier and E. I. Obiajunwa, Nucl. Phys. **A500**, 323 (1989).
[7] J. Jabbour, L. H. Rosier, E. I. Obiajunwa, and B. Ramstein, Nucl. Phys. **A500**, 356 (1989).
[8] J. Cook, Nucl. Phys. **A388**, 153 (1982).
[9] G. B. Silva, Dissertação de Mestrado, IFUSP, 2000.
[10] M. D. L. Barbosa, Tese de Doutorado, IFUSP, 2001.
[11] S. Raman, C. W. Nestor, Jr., and P. Tikkanen, At. Data and Nucl. Data Tables **78**, 1 (2001).
[12] A. M. Bernstein, V. R. Brown, and V. A. Madsen, Phys. Lett. **B71**, 48 (1977); **B103**, 255 (1981).
[13] P. D. Kunz, computer code DWUCK4, University of Colorado, 1974.
[14] L. C. Gomes *et al*., Phys. Rev. C **54**, 2296 (1996).
[15] G. M. Ukita, T. Borello-Lewin, L. B. Horodynski-Matsushigue, J. L. M. Duarte, and L. C. Gomes, Phys. Rev. C **64**, 014316 (2001).
[16] L. B. Horodynski-Matsushigue, T. Borello-Lewin, and J. L. M. Duarte, in Proceedings of the International Nuclear Physics Conference, São Paulo, Brazil, 1989, Vol. I, p. 307.
[17] D. J. Horen, G. R. Satchler, S. A. Fayans, and E. L. Trykov, Nucl. Phys. **A600**, 193 (1996).
[18] H. T. Fortune and M. Carchidi, Phys. Rev. C **36**, 2584 (1987).
[19] D. Ardouin, R. Tamisier, G. Berrier, J. Kalifa, G. Rotbard, and M. Vergues, Phys. Rev. C **11**, 1649 (1975).
[20] H. T. Fortune *et al*., Phys. Rev. C **35**, 1603 (1987).
[21] M. Carchidi, H. T. Fortune, G. S. F. Stephans, and L. C. Bland, Phys. Rev. C **30**, 1293 (1984).
[22] M. Carchidi, H. T. Fortune, and M. Burlein, Phys. Rev. C **39**, 795 (1989).
[23] M. Carchidi and H. T. Fortune, Phys. Rev. C **31**, 853 (1985).
[24] R. Lecomte, M. Irshad, S. Landsberger, G. Kajrys, P. Paradis, and S. Monaro, Phys. Rev. C **22**, 2420 (1980).
[25] R. Lecomte, G. Kajrys, S. Landsberger, P. Paradis, and S. Monaro, Phys. Rev. C **25**, 2812 (1982).
[26] F. Guilbault, D. Ardouin, J. Uzureau, P. Avignon, R. Tamisier, G. Rotbard, M. Vergnes, Y. Deschamps, G. Berrier, and R. Seltz, Phys. Rev. C **16**, 1840 (1977).
[27] A. C. Rester, J. B. Ball, and R. L. Auble, Nucl. Phys. **A346**, 371 (1980).
[28] R. Lecomte, M. Irshad, S. Landsberger, P. Paradis, and S. Monaro, Phys. Rev. C **22**, 1530 (1980).
[29] B. Kotlinski *et al*., Nucl. Phys. **A519**, 646 (1990).
[30] Y. Toh *et al*., Eur. Phys. J. A **9**, 353 (2000).
[31] Y. Toh *et al*., J. Phys. G **27**, 1475 (2001).
[32] M. Sugawara *et al*., Eur. Phys. J. A **16**, 409 (2003).
[33] J. L. Wood, K. Heyde, W. Nazarewicz, M. Huyse, and P. Van Duppen, Phys. Rep. **215**, 101 (1992).
[34] P. Duval, D. Goutte, and M. Vergnes, Phys. Lett. **B124**, 297 (1983).
[35] S. T. Hsieh, H. C. Chiang, and Der-San Chuu, Phys. Rev. C **46**, 195 (1992).
[36] K. Kumar, J. Phys. G **4**, 849 (1978).
[37] A. Wolf, O. Scholten, and R. F. Casten, Phys. Lett. **B312**, 372 (1993).
[38] N. Kato, Nucl. Phys. **A203**, 97 (1973).